Cell Reports, Volume *17*

Supplemental Information

Differential Effects of Environmental and Genetic Factors on T and B Cell Immune Traits

Raul Aguirre-Gamboa, Irma Joosten, Paulo C.M. Urbano, Renate G. van der Molen, Esther van Rijssen, Bram van Cranenbroek, Marije Oosting, Sanne Smeekens, Martin Jaeger, Maria Zorro, Sebo Withoff, Antonius E. van Herwaarden, Fred C.G.J. Sweep, Romana T. Netea, Morris A. Swertz, Lude Franke, Ramnik J. Xavier, Leo A.B. Joosten, Mihai G. Netea, Cisca Wijmenga, Vinod Kumar, Yang Li, and Hans J.P.M. Koenen

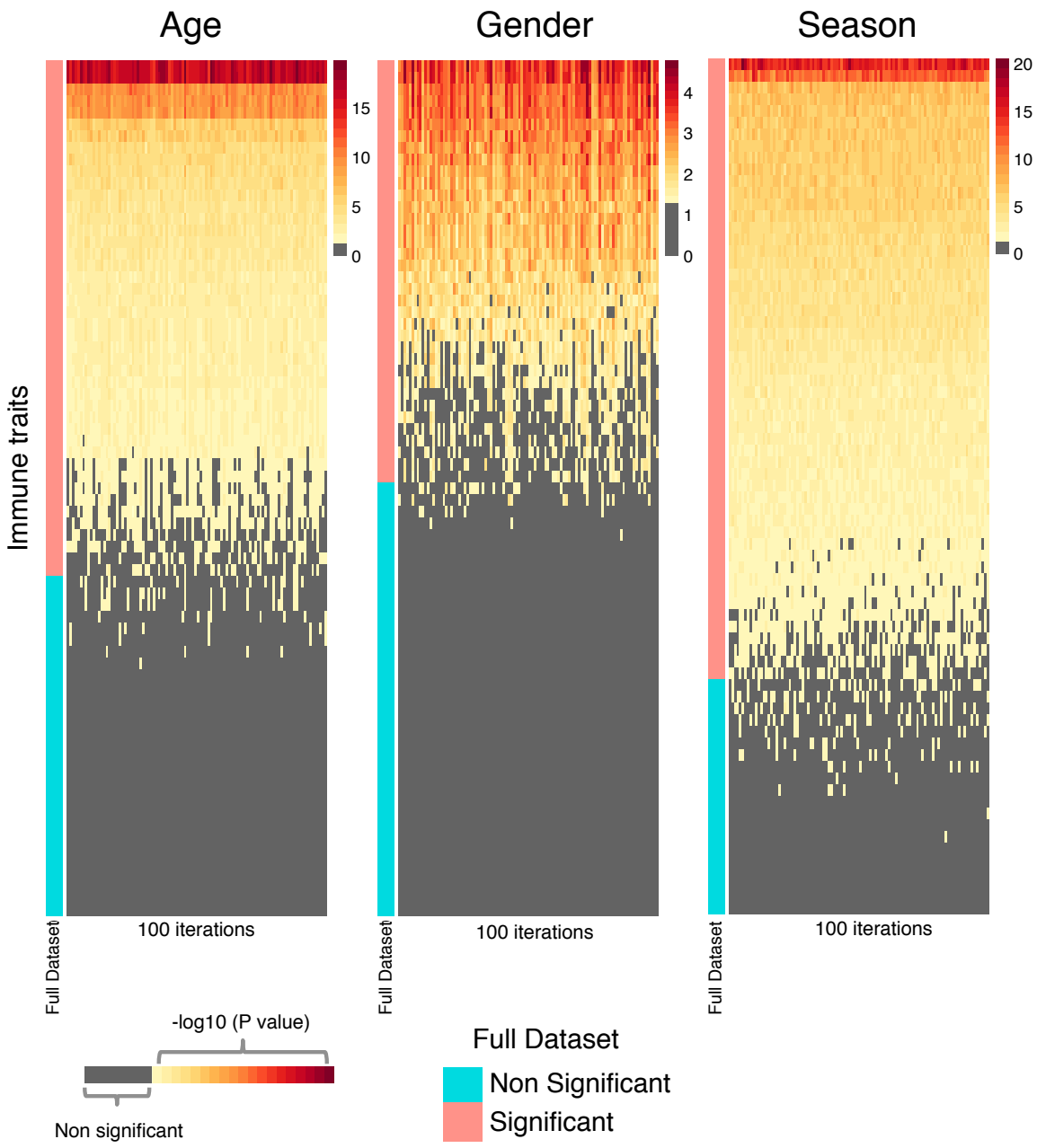

Figure S1: Robustness of age, gender and season effect on immune traits. (Related to Figure 3). We randomly selected 90% of all the samples and performed statistical tests for each different type of association. For the age effect on immune traits we used the Spearman correlation; for the gender effect on immune traits we used a t-test; and for the seasonal effect on immune traits we used a cosinor model. We repeated this 100 times and show the statistical significance for each test (-log10 P value) using gradient colour. In each panel, the rows represent the immune traits, and the columns represent each individual resampling. We counted the number of traits that show consistent results when compared with the original full dataset in more than 70% of the sampling. In this way we could reproduce 91% of all the immune traits of the age effects, 87% of the gender effects and 94% of the seasonal effects.

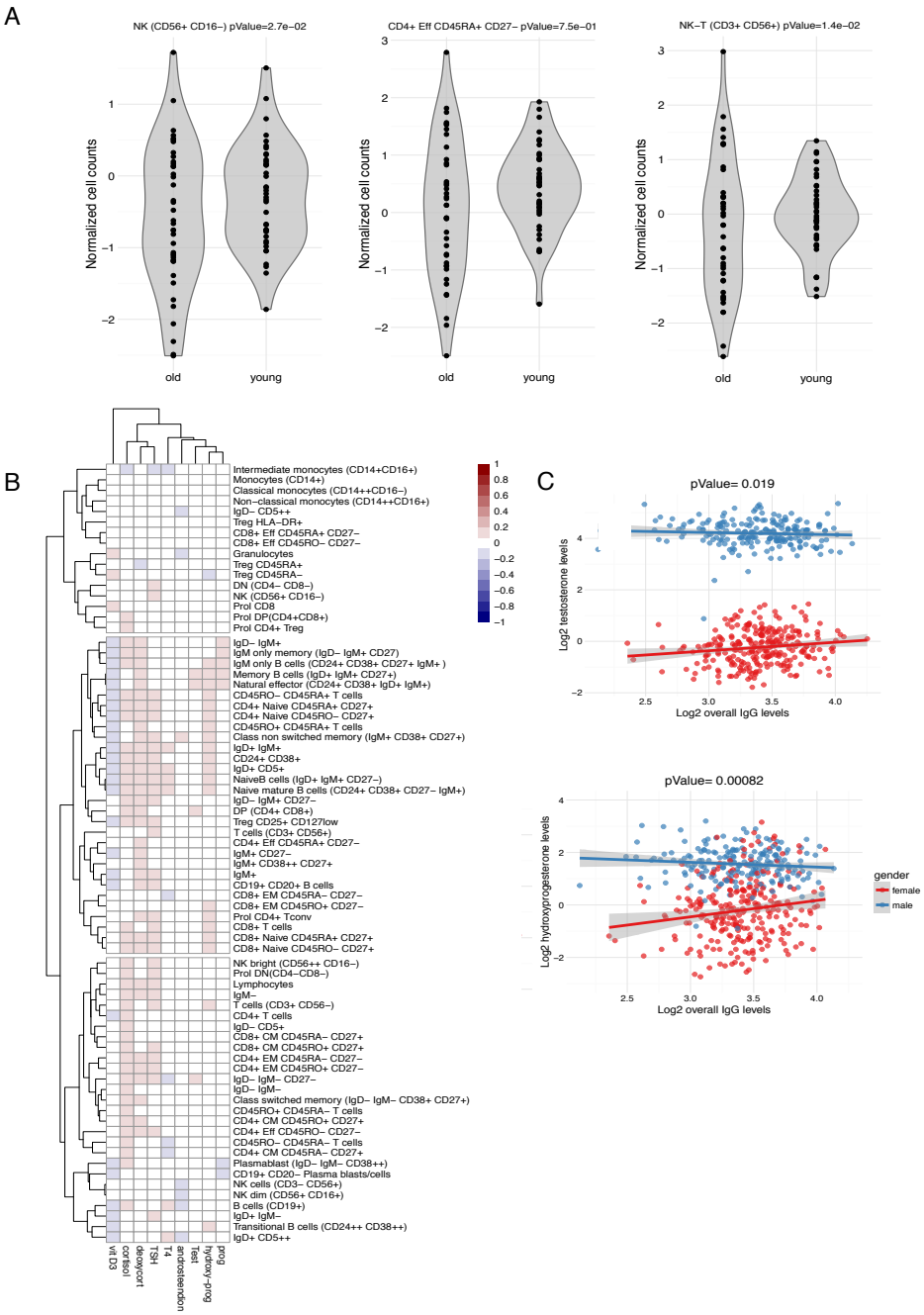

Figure S2: Immune traits can be modulated by non-heritable factors. (Related to Figure 3)(A) Variation of cell levels comparing the oldest and youngest volunteers from our cohort. (B) Hierarchical clustering of the correlation between hormones and cell levels in the 500FG cohort. (C) Correlation of testosterone (upper panel) and 17-hydroxyprogesterone (lower panel) levels with IgG levels in males versus females. .

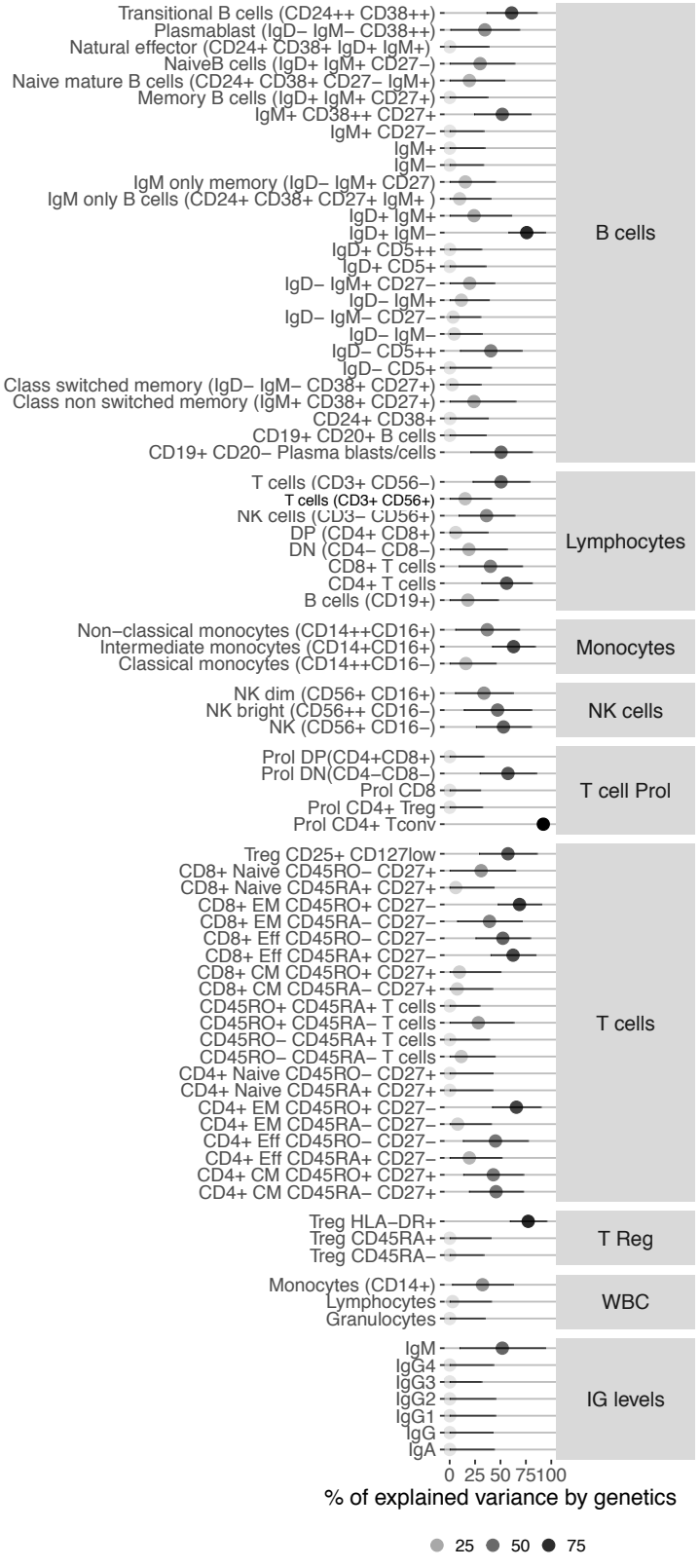

Figure S3: Proportion of variance explained by genetics in each of the 73 independent cell types. (Related to Figure 4)

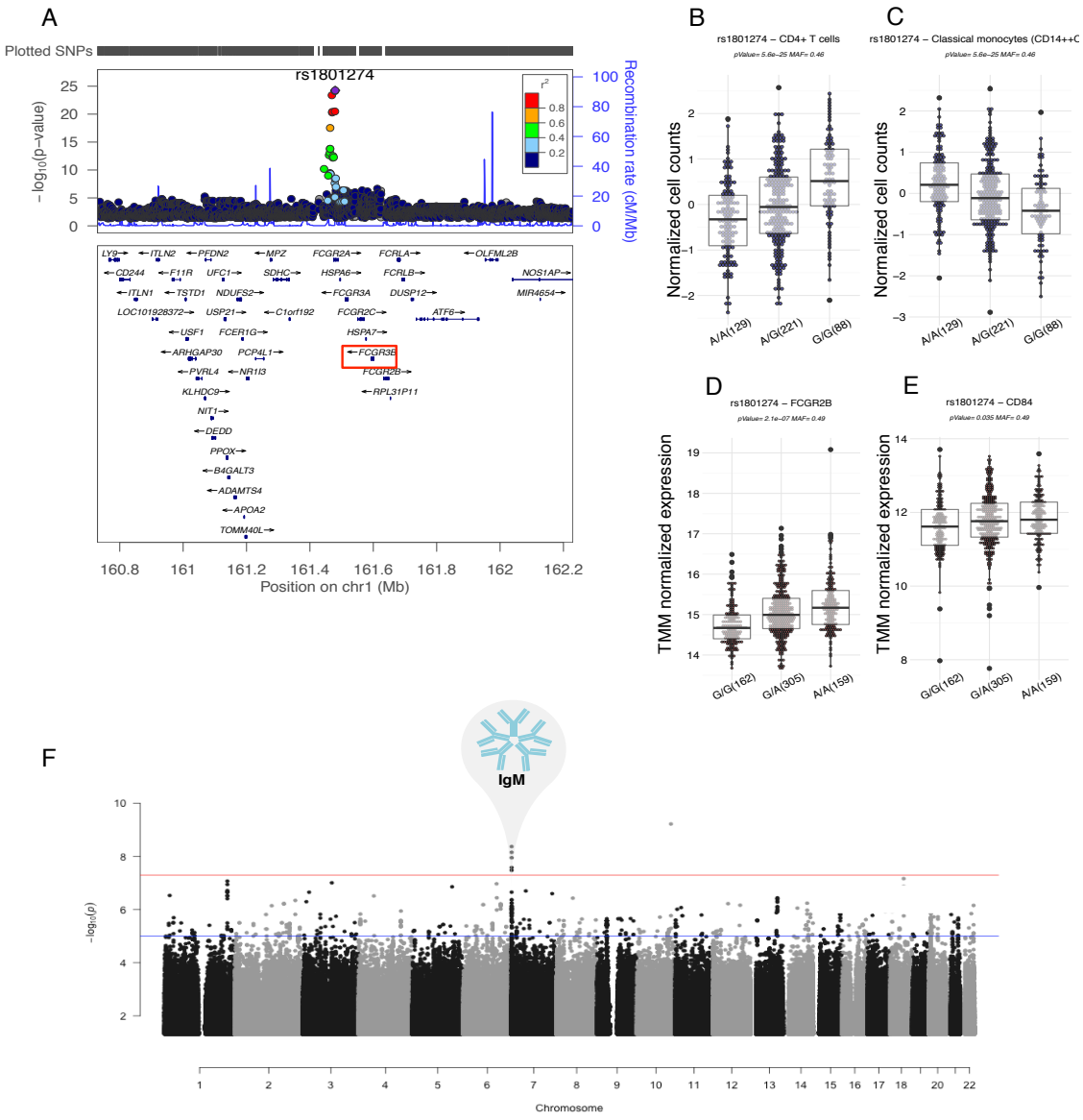

Figure S4: Combined Manhattan plot of immunoglobulin levels associations with genotypes and the ccQTL in the FC locus has been previously reported in two independent studies. (Related to Figure 4). (A) One genome-wide significant Ig associated locus (rs62433089, P < 5E−08) was detected with a MAF ≥ 0.01. (B) A regional plot of the ccQTL located in the FC cluster. (C) and (D) ccQTLs box plots for CD4+ T cells and for classic monocytes, respectively. (E) and (F) cis expression QTL plots from the TC locus based on ~600 RNA-seq blood samples.

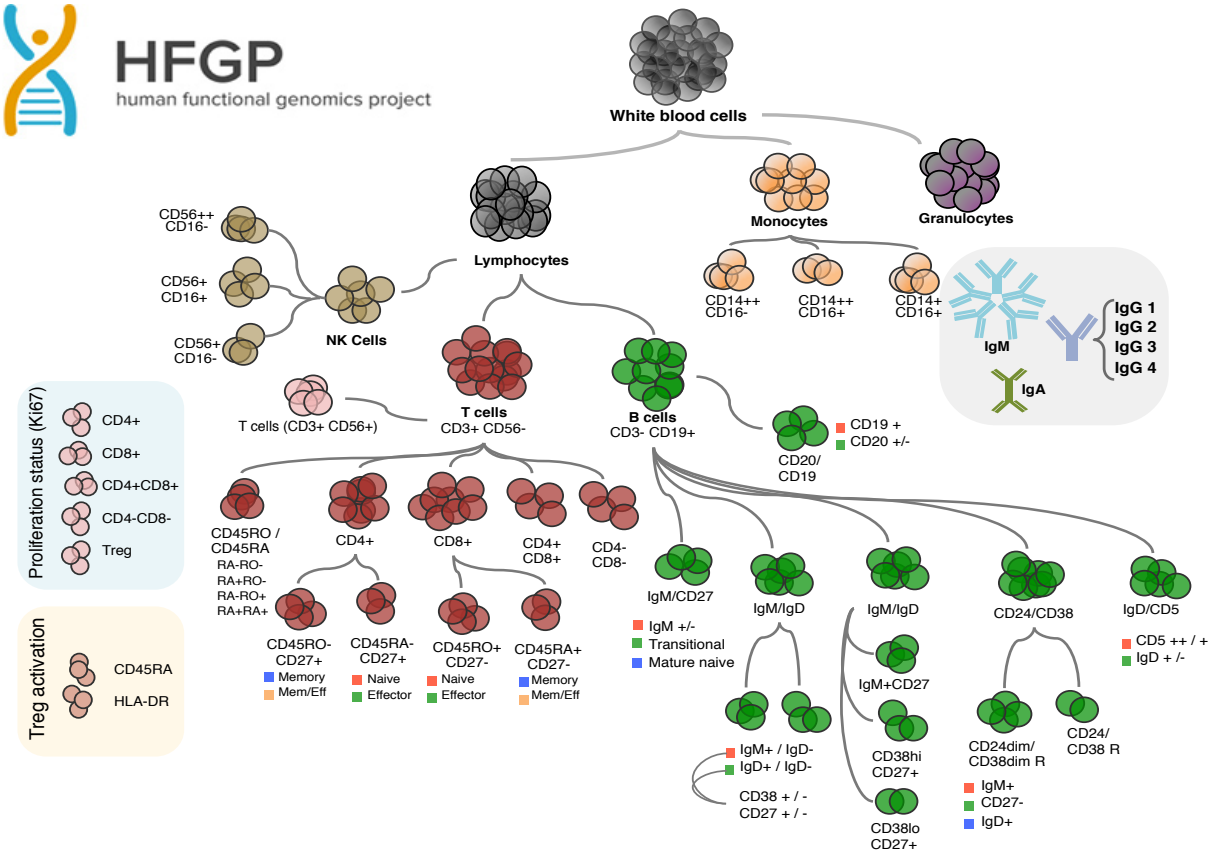

Figure S5: Immune cell subpopulations and serum immunoglobulin levels studied in the human functional genomics project. (Related to Figures 1-6) Schematic representation of the cell subpopulations and immunoglobulin subclasses quantified in the 500FG cohort. In freshly drawn blood samples, myeloid cells (granulocytes, monocyte subsets) and lymphoid immune cells (T cell subsets, B cell subsets, NK cells, CD3+ CD56+ T cells) were analysed by 10-color flow cytometry. Serum immunoglobulin levels were analysed by fluorescence enzyme immunoassay (FEIA).

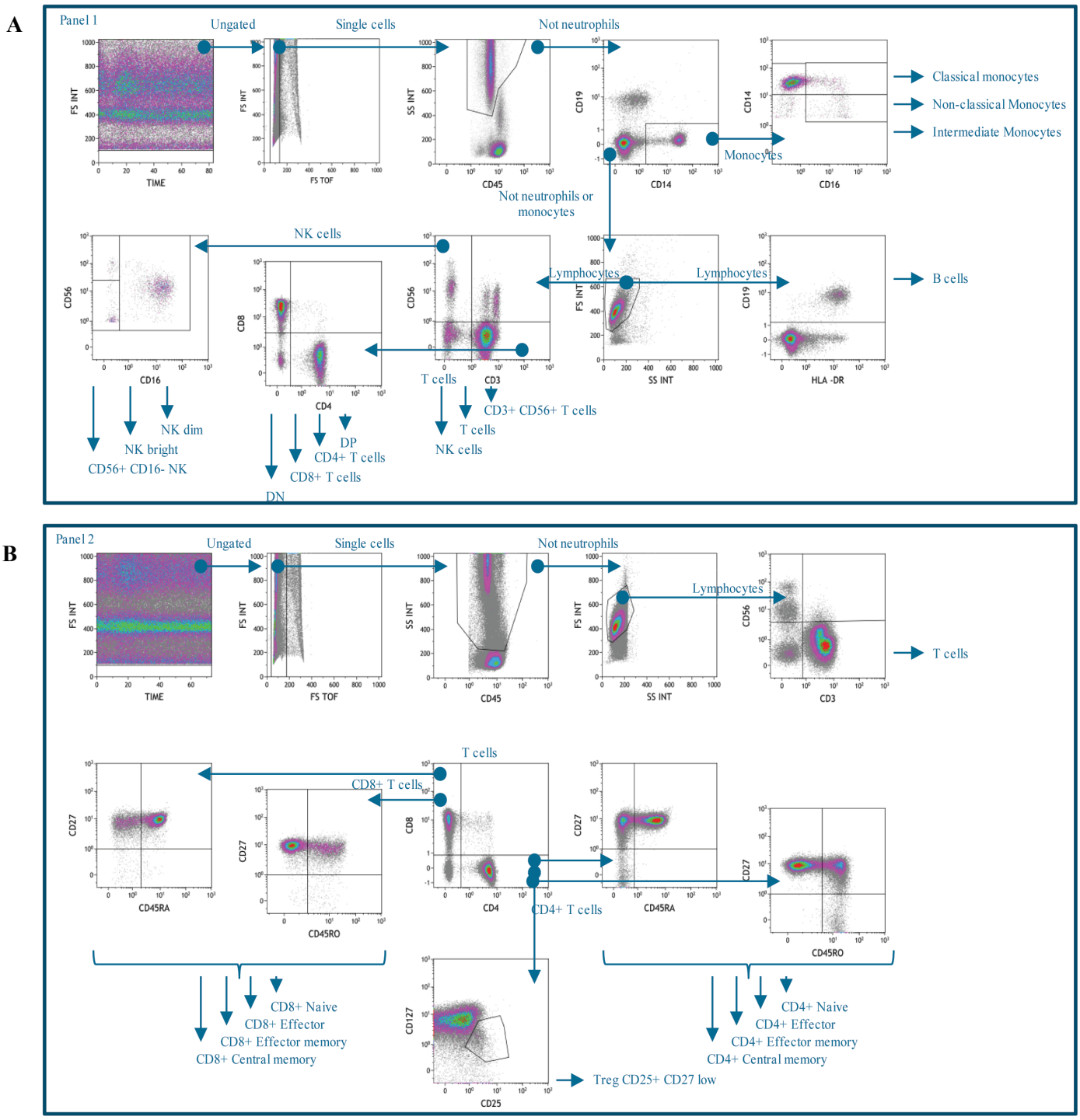

Figure S6: Flow cytometry gating strategy of the general (A) and T cells (B) panel. (Related to Figures 1-6)

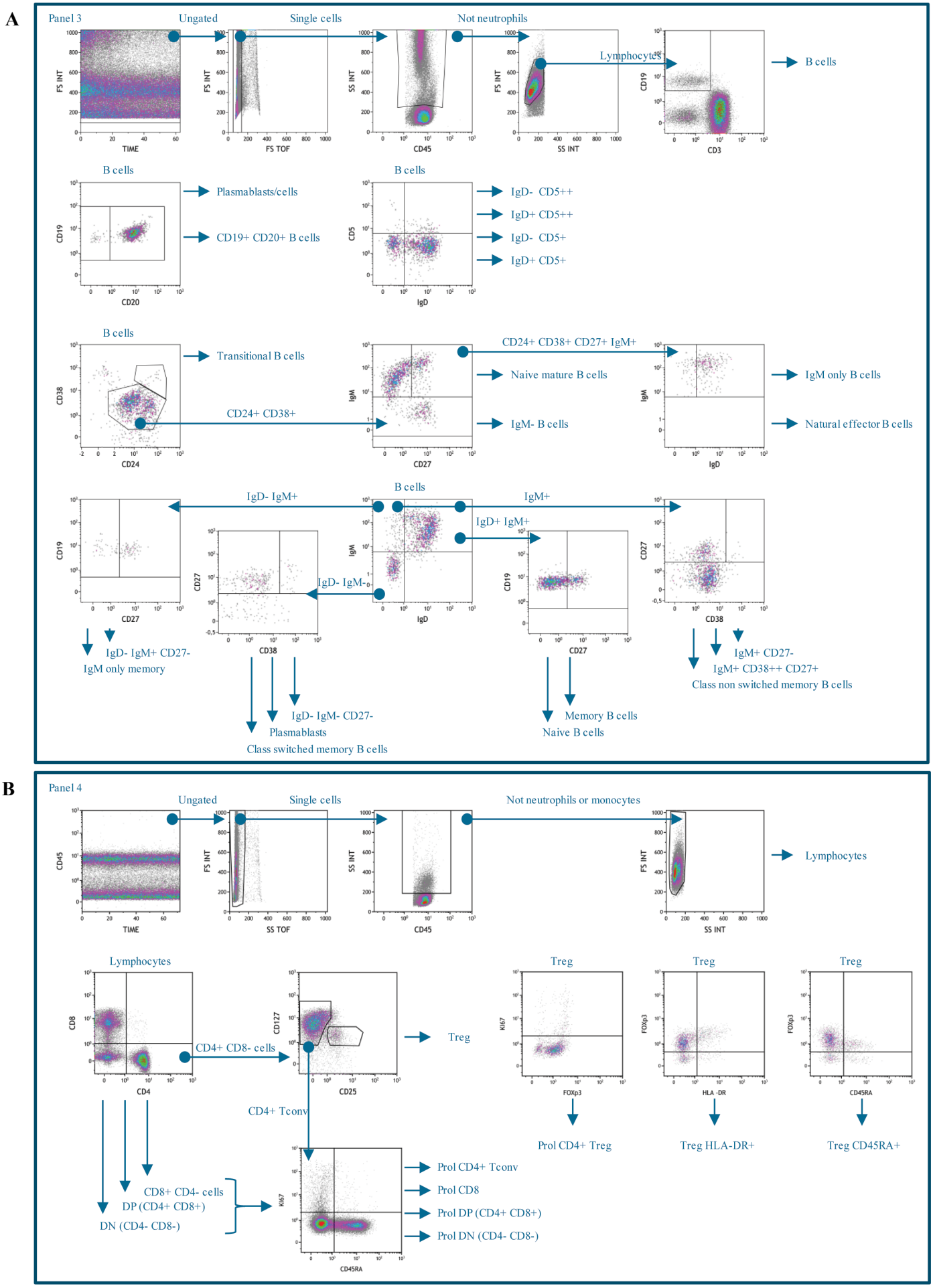

Figure S7: Flow cytometry gating strategy for the B cell (A) and intracellular Tcell/Treg (B) panel.
(Related to Figures 1-6)

Table S3. Table of GW significant loci and all the cell subpopulations which had either a GWA p-Value or a suggestive p-Value (<= $1x10^{-6}$)

SNP	CHR	BP	ccQTL P[1]	GW significantly associated cell types	Suggestively associated traits *
rs1801274	1	161479745	5.60E-25	%P_T cells (CD3+ CD56-),%G_CD4+ T cells,%G_CD8+ T cells,%G_NK bright (CD56++ CD16-),%P_CD45RO- CD45RA+ T cells,%P_Treg CD25+ CD127low,%G_Treg CD25+ CD127low,%P_CD4+ Naive CD45RA+ CD27+,%G_CD4+ Naive CD45RA+ CD27+,%G_CD4+ CM CD45RA- CD27+,%P_CD4+ Naive CD45RO- CD27+,%G_CD4+ Naive CD45RO- CD27+,%P_CD4+ CM CD45RO+ CD27+,%G_CD4+ CM CD45RO+ CD27+,%P_CD8+ Naive CD45RA+ CD27+,%P_CD8+ Naive CD45RO- CD27+,Non-classical monocytes (CD14++CD16+),%P_Classical monocytes (CD14++CD16-),%P_Non-classical monocytes (CD14++CD16+),%G_Non-classical monocytes (CD14++CD16+)	%P_Treg CD25+ CD127low
rs72744884	2	241782823	2.20E-09	CD4+ EM CD45RO+ CD27-	CD4+ EM CD45RA- CD27-
rs153414	5	153748732	3.60E-08	CD4+ Tcells, Monocytes (CD14+)	Monocytes (CD14+),CD45RO- CD45RA+ T cells
rs10277809	7	44948953	2.80E-08	IgM only B cells (CD24+ CD38+ CD27+ IgM+)	IgM only memory (IgD- IgM+ CD27)
rs2707213	12	6899181	1.30E-09	%P_DP (CD4+ CD8+),%G_DP (CD4+ CD8+),DP (CD4+ CD8+)	
rs7403546	15	87871288	2.30E-08	Class non switched memory (IgM+ CD38+ CD27+)	
rs2164983	19	8789381	2.70E-08	%G_NK bright (CD56++ CD16-)	%P_Memory B cells (IgD+ IgM+ CD27+)
rs280499	19	10489606	5.70E-09	CD8+ CM CD45RO+ CD27+	CD8+ CM CD45RA- CD27+

* Nominal p-value <= $1x10^{-5}$

Table S4. 10 colour flow cytometry panels used in the FG500 study. Samples were analysed by a 3-laser Navios (Beckman Coulter)

***(ic); intracellular staining**

	Flow channel	FL1	FL2	FL3	FL4	FL5	FL6	FL7	FL8	FL9	FL10
General panel	whole blood	CD16	HLA-DR	CD14	CD4	CD25	CD56	CD8	CD19	CD3	CD45
		3G8	immu-357	UCHT1	13B8.2	M-A251	N901	B9.11	J3-119	UCHT1	J33
		Coulter	Coulter	Coulter	Coulter	BD	Coulter	Coulter	Coulter	Coulter	Coulter
	fluorochrome	**FITC**	**PE**	**ECD**	**PE-Cy5.5**	**PC7**	**APC**	**APC-AF700**	**APC-AF750**	**PB**	**KO**
T cell panel	whole blood	CD45RA	CD3	CD45RO	CD27	CD25	CD56	CD127	CD8	CD4	CD45
		ALB11	UCHT1	UCHL1	1A4CD27	M-A251	N901	R34.34	B9.11	13B8.2	J33
		Coulter	Coulter	Coulter	Coulter	BD	Coulter	Coulter	Coulter	Coulter	Coulter
	fluorochrome	**FITC**	**PE**	**ECD**	**PE-Cy5.5**	**PC7**	**APC**	**APC-AF700**	**APC-AF750**	**PB**	**KO**
B cell panel	whole blood	IgD	IgM	CD3	CD27	CD38	CD24	CD5	CD19	CD20	CD45
		IADB6	SA-DA4	UCHT1	1A4CD27	LS198-4-3	ALB9	BL1a	J3-119	B9E9	J33
		Coulter	Coulter	Coulter	Coulter	Coulter	Coulter	Coulter	Coulter	Coulter	Coulter
	fluorochrome	**AF488**	**PE**	**ECD**	**PE-Cy5.5**	**PC7**	**AF647**	**APC-AF700**	**APC-AF750**	**e450**	**KO**
T cell division / Treg panel	PBMC	KI67 (ic)*	HLA-DR	CD45RA	CD4	CD25	Helios (ic)	CD127	CD8	FoxP3 (ic)	CD45
		B56	immu-357	2H4LDH11LDB9	13B8.2	M-A251	22F6	R34.34	B9.11	PCH101	J33
		BD	Coulter	Coulter	Coulter	BD	Biolegend	Coulter	Coulter	eBiocience	Coulter

Supplemental Figures

Figure S1: Robustness of age, gender and season effect on immune traits. (Related to Figure 3)**.** We randomly selected 90% of all the samples and performed statistical tests for each different type of association. For the age effect on immune traits we used the Spearman correlation; for the gender effect on immune traits we used a *t*-test; and for the seasonal effect on immune traits we used a cosinor model. We repeated this 100 times and show the statistical significance for each test (-log10 P value) using gradient colour. In each panel, the rows represent the immune traits, and the columns represent each individual resampling. We counted the number of traits that show consistent results when compared with the original full dataset in more than 70% of the sampling. In this way we could reproduce 91% of all the immune traits of the age effects, 87% of the gender effects and 94% of the seasonal effects.

Figure S2: **Immune traits can be modulated by non-heritable factors.** (Related to Figure 3)**(A)** Variation of cell levels comparing the oldest and youngest volunteers from our cohort. **(B)** Hierarchical clustering of the correlation between hormones and cell levels in the 500FG cohort. **(C)** Correlation of testosterone (upper panel) and 17-hydroxyprogesterone (lower panel) levels with IgG levels in males versus females.

Figure S3: Proportion of variance explained by genetics in each of the 73 independent cell types. (Related to Figure 4)

Figure S4: Combined Manhattan plot of immunoglobulin levels associations with genotypes and the ccQTL in the FC locus has been previously reported in two independent studies. (Related to Figure 4). **(A)** One genome-wide significant Ig associated locus (rs62433089, $P < 5E{-}08$) was detected with a MAF ≥ 0.01. **(B)** A regional plot of the ccQTL located in the FC cluster. **(C)** and **(D)** ccQTLs box plots for CD4+ T cells and for classic monocytes, respectively. **(E)** and **(F)** *cis* expression QTL plots from the TC locus based on ~600 RNA-seq blood samples.

Figure S5: Immune cell subpopulations and serum immunoglobulin levels studied in the human functional genomics project. (Related to Figures 1-6) Schematic representation of the cell subpopulations and immunoglobulin subclasses quantified in the 500FG cohort. In freshly drawn blood samples, myeloid cells (granulocytes, monocyte subsets) and lymphoid immune cells (T cell subsets, B cell subsets, NK cells, CD3+ CD56+ T cells) were analysed by 10-color flow cytometry. Serum immunoglobulin levels were analysed by fluorescence enzyme immunoassay (FEIA).

Figure S6: Flow cytometry gating strategy of the general (A) and T cells (B) panel. (Related to Figures 1-6)

Figure S7: Flow cytometry gating strategy for the B cell (A) and intracellular Tcell/Treg (B) panel. (Related to Figures 1-6)

Supplemental Tables

Table S1: Summary statistics for all cell counts and immunoglobulin level associations. (Related to Figure 1). (Excel file)

Table S2: Summary statistics for all associations of cell counts and immunoglobulin levels with age, gender and season. (Related to Figure 3) (Excel file)

Table S3: Table of GW significant loci and all the cell subpopulations which had either a GWA p-Value or a suggestive p-Value (<= $1x10^{-6}$). (Related to Table1)**.** (Word file)

Table S4: 10 colour flow cytometry panels used in the 500FG study. (Related to Figures 1-6. (Word file)

Table S5: Distribution of the 73 independent cell count levels before and after inverse rank transformation.(Related to Figures 1 and 3). (Excel file)

Extended experimental procedures

Immunophenotyping

Peripheral blood mononuclear cell isolation and staining

Blood was collected in 10 ml BD Vacutainer® spray-coated K2EDTA tubes. Fresh peripheral blood cells were counted using a Coulter Ac-T Diff® cell counter (Beckman Coulter, Brea, USA) that was calibrated daily. The absolute number of white blood cells (WBC) per ml of blood determined by the cell counter was used to calculate the absolute numbers of CD45+WBC cell subsets as measured by flow cytometry. As an example, WBC $8x10^6$/ml blood represents the CD45+ WBC as identified by flow cytometry, 5% CD14+ monocytes represent $0.4x10^6$ CD14+ monocytes/blood. Both erythrocyte-lysed whole blood samples (panel 1-3) and density gradient isolated PBMC (panel 4) were analyzed by flow cytometry.

Cell Processing (whole blood and PBMC)

1.5 ml whole blood was incubated in lysis buffer containing 3.0 M NH_4Cl, 0.2 M $KHCO_3$ and 2mM Na_4EDTA for 10 min to lyse erythrocytes. Remaining white blood cells were further diluted with 25 ml PBS (Braun, Melsungen, Germany) and spun down at 452 x g for 5 min at room temperature (RT). Cells were washed and spun down in PBS (Braun) once again and resuspended in 300 µl of PBS + 0.2% BSA (Sigma-Aldrich, Zwijndrecht, Netherlands). 100 µl was transferred for surface staining to each of 3 wells of a 96 well v-bottom plate (Greiner Bio-One, Frickenhausen, Germany).

For PBMC isolation 8.5 ml of whole blood was placed on top of a density gradient layer (Lymphoprep™, Axis-Shield, Oslo, Norway) and centrifuged at 804 x g for 20 minutes at RT, no brake. Interphase containing purified PBMC was transferred to a new tube and washed twice with PBS at 452 x g for 5 minutes. Cells were resuspended in PBS and cell count was performed. For staining 0.5 x 10^6 cells were transferred to 1 well of a 96 well v-bottom plate.

Reagents

Table S3 shows the fluorochrome conjugate and clone identity of the antibodies that were used in the antibody panels. Immunofluorescence reagents used to generate the panel master mixes were purchased from Beckman Coulter (Marseille, France), Becton Dickinson (San Jose, USA), eBioscience (Vienna, Austria) or BioLegend (San Diego, USA). All reagents were titrated and tested before they were used in the current study.

Staining

All cells were surface stained in 25 µl of surface staining master mix at RT for 20 minutes. Cells were washed twice by adding PBS + 0.2% BSA and centrifuged at 250 x g for 2.5 min. Buffer was removed by flicking the plates. Before acquisition, whole blood derived cells were resuspended in 100 µl PBS + 0.2% BSA.

For intracellular staining, the surface stained PBMC were fixed and permeabilized using Fix/Perm solution (eBioscience, Vienna, Austria). After 30 minutes at 4°C protected from light, cells were washed and centrifuged at 250 x g for 2.5 min twice using permeabilisation buffer (eBioscience, Vienna, Austria). Then, 25 µl of intracellular staining master mix was applied and the samples were incubated for 30 minutes at 4°C protected from light. After a second washing step using permeabilisation buffer, cells were resuspended in 100 µl PBS + 0.2% BSA for data acquisition.

Gating strategy

Each sample was analyzed by four 10-color antibody panels: 1. general, 2. T cell, 3. B cell and 4. intracellular T cell/Treg. Gating strategy and example stainings are illustrated in **Figure S6** and **S7.**

For every panel, the single cells within the leukocyte (CD45+) population were first gated and thereafter the major myeloid or lymphoid lineages identified. Single cells were identified by plotting the FS Time Of Flight (FS TOF) against FS. Given that single leukocytes need a well defined period of time to pass the laser, this parameter can be used to identify single cells. The first 178 out of 516 samples included did not include the TOF parameter. In these samples the leukocyte population was gated on the CD45+ leucocytes.

In panel 1, granulocytes and lymphocytes were discriminated by forward scatter and side scatter, while monocytes were characterized by CD14 expression. Within the lymphocytes, T cells (CD3+, CD56-), NK cells (CD3-, CD56+), CD3+ CD56+ T cells and B cells (CD19+, HLA-DR+) were characterized. Subpopulations within T cells, NK cells and monocytes were analyzed by CD4 and CD8, CD56 and CD16, and CD14 and CD16 expression, respectively.

In panel 2, CD4+ regulatory T cells (Treg, CD4+, CD25+ CD127 low) and CD45RA/CD27 and CD45RO/CD27 maturation stages of CD4 and CD8 T cells were identified.

Panel 3 aimed to define CD19+ B cell maturation stages by the expression of IgM/IgD and/or CD24/CD38 expression as proposed previously (Berkowska et al., 2011; Wehr et al., 2008). B cell subsets were additionally identified by differential CD19/CD20 and IgD/CD5 expression. Although it may identify redundant B cell

populations, we decided to use different multiple gating strategies to cover most of the B cell subpopulations that have been described.
In panel 4, the major T cell populations (CD4, CD8 and Treg) were identified and subsequently analyzed for proliferation status by intracellular Ki67 expression. Treg (CD4+, CD25+ CD127low FOXP3+) were analyzed for expression of CD45RA and HLA-DR. Absolute cell counts in panel 4 (PBMC obtained after density gradient isolation) were calculated as described above taking into account the whole blood cell counts minus the granulocyte number as determined in panel 1. Variability in the median fluorescence intensity of the immune markers during the 1.5 year acquisition period was low (%CV of all markers ranges from 0.15–0.38, %CV for CD16 = 0.53). In case of a limited number of specimens the pre-defined gate setting was slightly modified as biological variation sometimes seems to influence forward and side scatter (FSC and SSC, resp.). In a minor number of specimens biological variation led to altered expression of lineage markers (e.g. CD56/CD3). In these cases, the marker settings were adjusted. We did not observe significant batch effect association of age and sex when testing against the month of collection (data not shown).

Flow cytometry measurements and data analysis
Data were acquired with a Navios Flow Cytometer as described above. Each sample suspended in 100 µl was measured for 60 seconds representing 75% of the sample volume. This prevented the intake of air leading to a nonspecific signal at the end of measurement. For the flow cytometry analysis a manual gating strategy was conducted. Each analysis was verified by two independent specialists to prevent gating errors. Analysed data was stored batch wise per 20 samples each. The statistics were exported batch wise for further analysis.

Serum Immunoglobulin levels
Serum levels of IgG, IgM and IgA were determined by immunonephelometry using a Beckman Coulter Immage (Beckman Coulter, Fullerton, CA, USA) and Beckman Coulter reagents. Measurements were standardized using certified European reference material 470 (ERM®-DA470). Reference values for serum Ig are: total IgG_2 7.0-16 g/l; IgM, 0.4-2.3 g/l; and IgA, 0.7-4.0 g/l. IgG subclass measurements were performed in serum on a BN™ II immunonephelometer (Siemens Healthcare, Erlangen, Germany) using the Binding Site© (Birmingham, UK) Human IgG Subklass BN II Combi Kit. Values were standardized using the N protein standard SL (OQIM, Siemens Healthcare), which is based on the Sanquin (Amsterdam, Netherlands) nephelometric standard M1590. Reference values are: IgG1 4.9-11.4 g/l, IgG2 1.5-6.4 g/l, IgG3 0.2-1.1 g/l and IgG4 0.08-1.4 g/l.

Serum hormone levels
Free Thyroxin (FT4 gen II) and TSH were analysed on a Modular E170 random access analyzer (Roche Diagnostics, Mannheim).

Vitamin D measurements
25-hydroxy vitamin D3 (25OH-vitamin D3) was analysed by liquid chromatography-tandem mass spectrometry after protein precipitation and solid-phase extraction. Internal standard [^{2}H3] 25OH-vitamin D_3 (Bioconnect) was added to 100 µL serum. 50 µL NaOH (2M) was added to release protein-bound 25OH-vitamin D_3 and 500 µL Acetonitrile/Methanol (9:1) was subsequently added for protein precipitation. 700 µL H_2O was added to 400 µL supernatant followed by solid phase extraction (Oasis HLB 1cc, Waters). Columns were conditioned with 1 mL methanol/isopropanol (95:5) and subsequently washed with 1 mL H_2O. After application of the sample, columns were washed with 1 mL H_2O and 1 mL methanol/H_2O (60:40). The eluate (300 µL methanol/isopropanol 95:5) was diluted with H_2O (3:1) and injected (10 µL) into an Agilent Technologies 1290 Infinity VL ultra high performance liquid chromatography-system (Agilent Technologies, Santa Clara, CA) equipped with a BEH C18 (1.7µm 2.1 X 50mm) analytical column (Waters Corp.) at 45°C. Mobile phase A (methanol:water 20:80 + 2 mM NH_4CH_3COO + 0.1% formic acid) and B (methanol:water 98:2 + 2 mM NH_4CH_3COO + 0.1% formic acid) were run in a gradient (0.4 mL/min). The gradient program was as follows: Start gradient 30:70 A:B to 5:95 A:B in 3.5 min and return to 30:70 A:B in 0.5 min. Retention time was 2.73 min. Total run time was 4 minutes. An Agilent 6490 tandem mass spectrometer (Agilent Technologies) was operated in the electrospray positive ion mode with a capillary voltage 3.5 kV, fragmentor voltage 380 V, sheath gas temperature 350 °C and gas temperature 100 °C with N_2 collision gas. Both 25OH-vitamin D_3 and 25OH-vitamin D_3 [-H_2O] (in-source fragmentation) were used for quantification (results were averaged) with both transitions (qualitative and quantitative) monitored. Transitions (Q1>Q3) were m/z 401.4 > 159.1 (27 kEV) and m/z 401.4 > 107.1 (27 kEV) for 25OH-vitamin D_3; m/z 404.4 > 109.1 (27 kEV) and m/z 404.4 > 162.1(30 kEV) for [$^2H_3$] 25OH-vitamin D3; m/z 383.4 > 107.1 (36 kEV) and m/z 383.4 > 257.2 (16 kEV) for 25OH-vitamin D_3 [-H_2O]; m/z 386.4 > 109.1 (27 kEV) and m/z 386.4 > 162.1 (27 kEV) for [^{2}H3] 25OH-vitamin D_3 [-H_2O]. Dwell time was 25 ms. An 8-point calibration curve was used, and the absolute concentration of the calibrator (Sigma-Aldrich) was assessed by spectrophotometry (264 nm). The method was linear assessed by CLSI EP6 protocol.

Recovery was between 90–109%. The within-run and between-run CV was 6.4% and 6.1% at 23 nmol/L and 5.1% and 5.5% at 81 nmol/L, as assessed by adapted CLSI EP5 protocol. LOQ was 7 nM (10% CV).

Steroid hormone measurements

Cortisol, 11-deoxycortisol, 17-hydroxyprogesterone, testosterone and progesterone were analysed by liquid chromatography-tandem mass spectrometry after protein precipitation and solid-phase extraction. Internal standard [$^{2}D_4$] cortisol, [^{2}D5] 11-deoxycortisol, [$^{14}C_3$] 17-hydroxyprogesterone, [$^{13}C_3$]-testosterone (Isoscience, King of Prussia, PA) and [$^{2}H_9$]-progesterone (CDN isotopes) was added to 100 µL serum. Subsequently, 300 µL Acetonitrile + 0.1% formic acid was added for protein precipitation. 300 µL H_2O was added to 200 µL supernatant followed by solid phase extraction (Oasis HLB 1cc, Waters). Columns were pre-equilibrated with 1 mL methanol:isopropanol (95:5) and subsequently washed with 1 mL H_2O. After application of the sample, columns were washed with 1 mL H_2O and 1 mL methanol/H_2O (30:70). The 300 µL eluate (methanol/isopropanol 95:5) was dried under a stream of N_2 gas, reconstituted in methanol:water (30:70) and injected (10 µL) into an Agilent Technologies 1290 Infinity VL ultra high performance liquid chromatography-system (Agilent Technologies, Santa Clara, CA) equipped with a BEH C18 (1.7µm 2.1 X 50 mm) analytical column (Waters Corp.) at 60°C. Mobile phase A (methanol:water 20:80 + 2 mM NH_4CH_3COO + 0.1% formic acid) and B (methanol:water 98:2 + 2 mM NH_4CH_3COO + 0.1% formic acid) were run in a gradient (0.4 mL/min). The gradient program was as follows: Start gradient 70:30 A:B for 2.5 min; then to 40:60 A:B in 3.5 min; followed by a gradient in 0.5 min to 2:98 to remain such for 0.5 min; and thereafter to 70:30 A:B in 0.5 min and remain such for 0.5 min. Retention time was 1.6 (cortisol), 2.8 (11-deoxycortisol), 4.4 (testosterone), 4.9 (17-hydroxyprogesterone) and 6.1 (progesterone) min with a total run time of 8 minutes. A 9-point calibration curve was used (cortisol, 11-deoxycortisol, testosterone, 17-hydroxyprogesterone (Steraloids); progesterone (Sigma)). An Agilent 6490 tandem mass spectrometer (Agilent Technologies) was operated in the electrospray positive ion mode, with a capillary voltage 3.5 kV, fragmentor voltage 380 V, sheath gas temperature 350°C and gas temperature 150 °C with N_2 collision gas. Two transitions (qualitative and quantitative) were monitored. Transitions (Q1>Q3), collision energy and dwell time were m/z 363.4 > 97.1 (34 kEV) and m/z 363.4> 121.1 (25 kEV) for cortisol (100 ms); m/z 367.4 > 97.1 (34 kEV) and m/z 367.4 > 121.1 (25 kEV) for [$^{2}D_4$] cortisol; m/z 347.2 > 109.1 (31 kEV) and m/z 347.2 > 97.1 (29 kEV) for 11-deoxycortisol (40 ms); m/z 352.3 > 113.1 (29 kEV) and m/z 352.3 > 100.1 (31 kEV) for [^{2}D5] 11-deoxycortisol. m/z 331.3 > 109.1 (31 kEV) and m/z 331.3 > 97.1 (31 kEV) for 17-hydroxyprogesterone (60 ms); m/z 334.3 > 112.1 (29 kEV) and m/z 334.3 > 100.1 (29 kEV) for [$^{14}C_3$] 17-hydroxyprogesterone; m/z 289.2 > 109.1 (30 kEV) and m/z 289.2> 97.1 (30 kEV) for testosterone (50 ms); m/z 292.3 > 112.1 (30 kEV) and m/z 292.3 > 100.1(30 kEV) for [$^{13}C_3$]-testosterone; m/z 315.3 > 109.1 (29 kEV) and m/z 315.3 > 97.1 (29 kEV) for progesterone (100 ms); m/z 324.3 > 113.1 (29 kEV) and m/z 324.3 > 100.1 (29 kEV) for [$^{2}H_9$]-progesterone. The method was linear for all steroids assessed by CLSI EP6 protocol. Recovery was 103% (cortisol), 97% (11deoxycortisol), 103% (17-hydroxyprogesterone), 98.4-103% (testosterone) and 99.8-102% (progesterone).

Within-run and between-run CV was assessed by adapted CLSI EP5 protocol. For cortisol within-run and between-run CV is 3.0% and 4.0% at 303 nmol/L and 2.5% and 3.4% at 1087 nmol/L. For 11-deoxycortisol, within-run and between-run CV is 4.8% and 6.6% at 2.1 nmol/L and 4.1% and 5.9% at 25.6 nmol/L. For 17-hydroxyprogesterone, within-run and between-run CV was 5.9% and 6.1% at 2.5 nmol/L and 4.9% and 5.1% at 91 nmol/L. For testosterone, within-run and between-run CV was 4.1% and 6.0% at 0.9 nmol/L and 3.3% and 5.3 at 19 nmol/L. For progesterone, within-run and between-run CV is 2.8% and 5.1% at 4.9 nmol/L and 3.4% and 6.1 at 28 nmol/L. LOQ was 0.10 nmol/L (10% CV), 0.10 nmol/ L (10% CV), 0.05 nmol/L (15% CV) and 0.25 nmol/ L (15% CV) for 11-deoxycortisol, 17-hydroxyprogesterone, testosterone and progesterone, respectively.

Statistical analysis

To test for association of cell counts or Ig levels with age, we normalized the immune traits as described above, then corrected for the effects of gender and season using a linear model. Using Spearman correlation analysis, we ascertained the significance and direction of the correlations. Significance was declared after controlling for multiple testing (FDR ≤ 0.05).

To test whether gender had any effect on the inter-individual variation of the immune traits, we used the cell counts normalized using an IRT and the log2 Igs levels, after correcting for the effect of age and season using a linear model. A paired T-test between the gender-stratified samples was carried out. Significance was declared after correcting for multiple testing (FDR ≤ 0.05).

To investigate the effect of season on the immune traits measured; we also made use of the IRT cell counts and log2 Igs levels. A cosinor model was fitted with the day of the year, in a one-year cycle period, using sex and age as covariates. The fitted model was compared with a reduced model without the season information and significance was ascertained (multiple correction testing; FDR ≤ 0.05) using a variance test between the full model (with season information) and the incomplete model (Dopico et al., 2015).